ACS APPLIED MATERIALS & INTERFACES

Research Article

www.acsami.org

Acid-Induced Release of Curcumin from Calcium Containing Nanotheranostic Excipient

Aifei Wang,[†] Faheem Muhammad,[†,‡] Wenxiu Qi,[‡] Nan Wang,[§] Liang Chen,[§] and Guangshan Zhu*[,†]

[†]State Key Laboratory of Inorganic Synthesis and Preparative Chemistry, College of Chemistry, and [‡]College of Life Science, Jilin University, Changchun 130012, China

[§]Department of Radiology, The First Hospital of Jilin University, Changchun 130012, China

Supporting Information

ABSTRACT: Poor water solubility is believed one of the most critical problems of numerous promising pharmaceutical ingredients in their successful clinical utilization. Nanomedicine holds considerable promise to address this challenge, because it extends the therapeutic window of hydrophobic drugs through nanonization approach. Recently, the integration of diagnostic agents with smart therapeutic nanocarriers is also an emerging research arena to simultaneously visualize diseased tissues, achieve site specific drug release and track the impact of therapy. In this study, we have developed a biocompatible smart theranostic nanosystem which transports a highly promising hydrophobic drug (curcumin) in response to mildly acidic environment. As calcium is a main constituent of human body, hence we exploited the reversible calcium chelate formation tendency of divalent calcium to load and unload curcumin molecules. Moreover, an emerging T1 contrast agent is also tethered onto the surface of nanocarrier to realize MRI diagnosis application. In-vitro cell experiments revealed a significantly high chemotherapeutic efficiency of curcumin nanoformulation (IC_{50}; 1.67 μg/mL), whereas free curcumin was found ineffective at the corresponding concentration (IC_{50}; 29.72 μg/mL). MR imaging test also validated the performance of resulting system. Our strategy can be extended for the targeted delivery of other hydrophobic pharmaceutical ingredients.

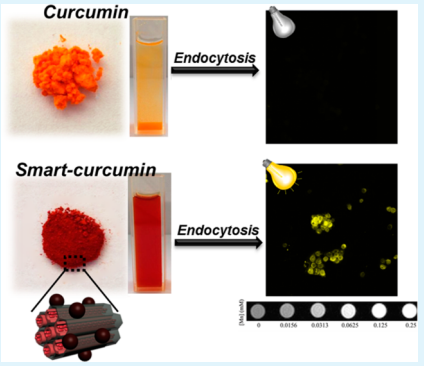

KEYWORDS: *curcumin, controlled release, pH responsive, theranostic, mesoporous silica*

INTRODUCTION

Over the last few decades, phenomenal developments in science and medicine have stimulated a rapid growth in discovery and screening of new active pharmaceutical ingredients (APIs), but unfortunately because of their poor solubility, a substantial number of promising APIs have been shelved. On average, more than 40% of newly discovered therapeutic candidates are found poorly water-soluble and this low water solubility consequently restricts their clinical use, since water insoluble drugs cannot reach at their site of action.[1] To surmount this obstacle, numerous efforts have so far been made to design water-soluble drug formulations. Chemical and physical modifications are generally explored as an alternative approaches to solubilize certain poorly water-soluble drugs.[2] The most effective physical modification strategy is the development of solid dispersions; in which the active therapeutic ingredients are dispersed in an appropriate carrier to improve solubility.[3,4] Similarly, chemical modifications such as structural alterations and prodrug formulations have also been tried,[5,6] however, API are mostly degraded or become pharmacologically inactive in these processes. A recent boom in nanotechnology has contributed a lot in all spheres of life. Medicine is no exception; it has extensively been demonstrated that nanonization of APIs can significantly improve the physical properties of drugs. In nanonization process, surface area to volume ratios and concentration gradient of poorly soluble APIs are significantly enhanced which in turn improve the drug solubility and pharmacokinetics.[7,8] Moreover, nanosized drug formulations also decrease the readily encountered systemic side effects through capitalizing EPR effect.[9,10] Considering positive aspects of nanosized drug formulations, the focus of nanomedicine in recent times is to develop such nanomaterial which can act as smart pharmaceutical excipient for targeted and controlled release of bioactive agents. To date, mostly organic-based carriers such as liposomes,[11,12] hydrogels,[13] surfactants,[14,15] and polymeric micelles[16] have been highlighted as nanocarriers to encapsulate hydrophobic APIs for improving water solubility, but poor chemical stability of organic-based carriers restricts their clinical utility, thus demands the development of more robust but biocompatible inorganic nanocarriers. In this regard, the high stability, biocompatible nature and large surface area of mesoporous silica nanoparticles (MSNs) make it a viable replacement to organic based carriers for entrapping poorly soluble APIs. Various hydrophobic drugs have been encapsulated into the unique porous architectures of MSNs; so far physical adsorption has been a main modus

Received: June 9, 2014
Accepted: July 15, 2014
Published: July 15, 2014

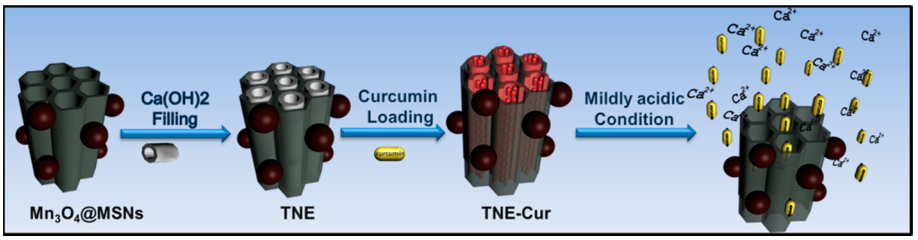

Figure 1. Schematic illustration of the formation of TNE, TNE loading with curcumin, and the pH stimuli responsive protocol.

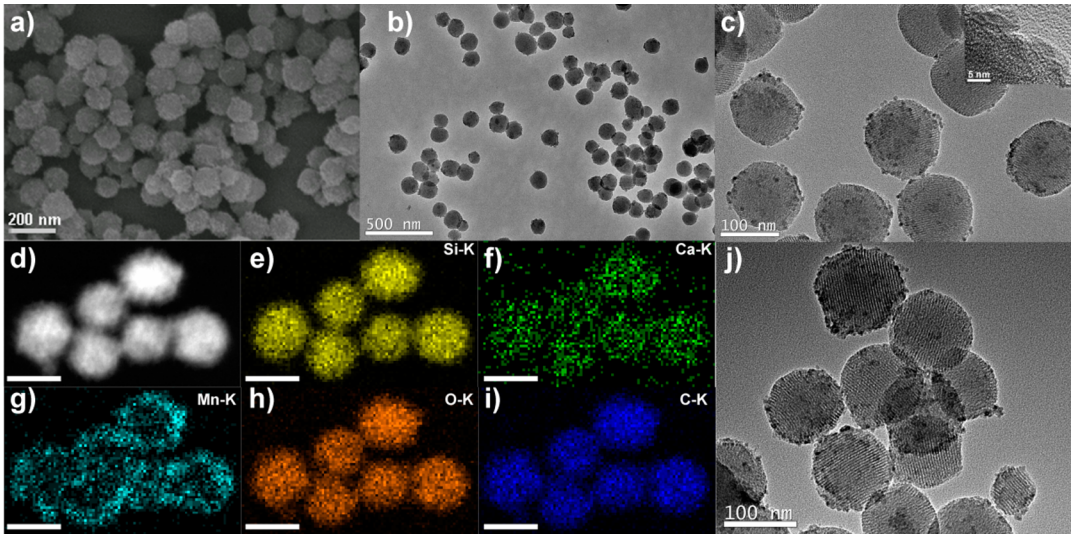

Figure 2. (a) SEM, (b) large-scale, and (c) TEM micrographs of Mn_3O_4 anchored MSNs and loading with $Ca(OH)_2$; inset in c is HRTEM images. (d–i) Images of high-angle annular dark-field scanning TEM and energy-dispersive X-ray elemental mapping of nanoexcipient. (j) TEM micrographs of the sample obtained of after incubation in weakly acidic solutions.

operandi to load hydrophobic drugs.[17−20] Curcumin is a promising hydrophobic which exhibits potent antioxidant, antiseptic, anti-inflammatory activities. Moreover, it also exhibits strong therapeutic activity against variety of cancers.[21−25] It is extremely safe even at a dosage as high as 12 g per day, but unfortunately, its safety therapeutic benefits could not be tapped because of extremely low water solubility (i.e., 0.0004 mg/mL at pH 7.3) and minimal systemic bioavailability. To overcome hydrophobicity, diverse kinds of curcumin formulations have been prepared, including nano-based liposomes,[26] proteins,[27] polymeric micelles,[28] and inorganic oxides.[29,30] Different mesoporous silica-based formulations have also been developed to enhance curcumin bioavailability. In a first attempt, curcumin was incorporated into CTAB micelle, during the formation of porous silica nanoparticles.[31] Later on, Jung and co-workers loaded covalently bonded curcumin into mesoporous hollow silica, using self-assembled alanine-based amphiphile.[32] Nevertheless, cumbersome synthetic procedures, bio irrelevant drug release conditions and toxicity CTAB limits the utility of those procedures. Besides mere drug delivery, the focus of nanomedicine is now being shifted to design theranostic nanocarriers, which combine diagnosis and therapy into a single nanoplatform for tracking the therapeutic efficacy of drug. Taken together, it remains a great challenge to fabricate theranostic nanocarrier with a high biocompatibility, enhanced drug loading, stimuli responsive release, and imaging functionality. Herein, we report a facile synthetic strategy to prepare highly biocompatible pH-responsive nanoexcipient for curcumin to improve the potency and biochemical attributes of hydrophobic drug. Moreover, T1 nanocontrast agent (Mn_3O_4) is integrated with curcumin nanocarrier to diagnose the disease or track the therapeutic effect of therapy. Synthetically, nanochannels of Mn_3O_4 conjugated MSNs (Mn_3O_4@MSNs) are filled with highly biocompatible calcium hydroxide and then curcumin is loaded via taking advantage of chelate forming ability of curcumin with divalent Calcium. Chemical loading enhances the apparent water solubility of curcumin due to amorphous state. Considering release of curcumin, both coordination bond and calcium hydroxide are disintegrated at mildly acidic conditions, and as a result drug molecules are readily unleashed in a burstlike fashion.

■ RESULTS AND DISCUSSION

The preparative and working protocol of nanotheranostic system for the delivery of curcumin is illustrated in Figure 1. MSNs nanoscaffold was initially synthesized according to a previously reported method. The diameter of as-synthesized MSNs was found to be ∼100 nm with MCM-41-type mesoporous structure. To tether Mn_3O_4 nanocrystals onto the outer surface MSNs, we functionalized the surface with carboxylic groups using succinic anhydride. On the other hand, aminopropyl-functionalized paramagnetic manganese oxide nanoparticles (Mn_3O_4 NPs) were synthesized using our newly developed facile and one-pot strategy. Mn_3O_4 NP synthesis and surface modification steps were carried out in N, N′-dimethylformamide (DMF), thus avoiding the use of toxic hydrophobic surfactants and laborious ligand exchange steps.

Later on, the resulting Mn_3O_4 NPs were assembled onto the surfaces of MSNs via direct EDC chemistry. As MSNs nanoparticles were functionalized with carboxylic groups, few of carboxyl groups were consumed during Mn_3O_4 immobilization, whereas the residual carboxylic groups in the silica matrix assisted the chemisorption of calcium ions (Ca^{2+}) and generation of $Ca(OH)_2$ within MSNs channels, following the treatment with NaOH. Finally, curcumin was loaded into the theranostic nanoexcipient (TNE-Cur) by simply mixing with the ethanolic solution of curcumin. Compared to previous reports, a significantly high loading amount of curcumin (180 mg/g) was achieved in this study.[17,31−34]

Scanning electron microscopy (SEM) and transmission electron microscopy (TEM) were applied to determine the morphology of the resulting TNE. In SEM micrograph, the size and structures of Mn_3O_4 anchored MSNs were retained after $Ca(OH)_2$ loading steps, as revealed in Figure 2 in which the average diameter of $Ca(OH)_2$ loaded spherical particle remain in the boundaries of ∼100 nm. Moreover, ultrasmall discrete dots were also observed onto the surface of porous silica, representing the successful immobilization of Mn_3O_4 nanoparticles. Similarly, TEM provided a bit more detailed picture at higher-resolution micrographs, as synthesized MSNs nanoparticles were found smooth surfaced with clear hexagonal nanochannels. On the contrary, the channel of MSNs became blurred due to the generation of $Ca(OH)_2$. Moreover, the outer surface of MSNs was also decorated with black dots because of the adherence of Mn_3O_4 nanoparticles onto the outer surface of MSNs. High resolution images (Figure 2c) apparently suggested the entrapment of $Ca(OH)_2$ in porous scaffold and successful doping of uniform Mn_3O_4 NPs (5 nm) around the MSNs matrix. Monodispersibility and uniformity is very important parameter in designing nanoexcipient, $Ca(OH)_2$ loading in our nanosystem did not lead to change in morphology of MSNs, neither aggregated product nor any extra $Ca(OH)_2$ formed outside. To further impart credibility to these observations, was also completed TEM-associated energy-dispersive spectroscopy (EDS) mapping analysis which revealed well-distributed Ca within MSNs matrix and partial Mn doping on outer surface. TEM investigation was also proven handy in probing the dissolution of pore entrapped $Ca(OH)_2$. As calcium compounds are susceptible in weakly acidic environ, therefore a shorter and mild acidic exposure resulted in the disintegration of encapsulated $Ca(OH)_2$. Figure 2j indicates that when TNPs-Cur were exposed to a slightly lower pH (pH 5.0) environment, the blurred mesoporous channels reemerged, suggesting the dissolution of $Ca(OH)_2$ in a mildly acidic environment.

X-ray powder diffraction (XRPD) analysis was performed to validate the presence of nanoexcipient encapsulation and curcumin loading using both small- and wide-angle techniques (Figure S1). In small-angle XRD, the intensity of characteristic MCM-41 type peak was markedly reduced in successive way after $Ca(OH)_2$ and curcumin inclusion, due to the generation of contrast and disordered product. To verify the possible changes in the crystalline nature of curcumin, wide-angle XRD analysis was done. Pure curcumin showed sharp peaks at 8.90, 12.26, 14.54, 17.24, 23.33, 24.60, and 25.52°, whereas the same drug-related prominent XRD patterns were completely disappeared in curcumin-loaded TNE, indicating an amorphous character of drug in the solid dispersion.[35,36] Such an amorphous modification of curcumin can be attributed to the suppression of its crystallization in the nanoconfinement of MSNs matrix and formation of complex with $Ca(OH)_2$. More interestingly, we also observed a clear chemical transformation in calcium hydroxide encapsulated MSN sample NE ($Ca(OH)_2$@MSNs). After a period of 2 months, few typical $CaCO_3$ peaks were emerged at ambient atmosphere, as can be seen in Figure S1c in the Supporting Information. In contrast, the curcumin-loaded sample revealed no such transformation, because curcumin-$Ca(OH)_2$ complex prevent transformation of $Ca(OH)_2$ to $CaCO_3$ and $Ca(OH)_2$ retains the amorphous phase in the curcumin-loaded sample. Furthermore, characteristics peaks of Mn_3O_4 also appeared in the wide-angle patterns, which implied the conjugation of paramagnetic contrast agents onto the outer surface of porous silica.

To probe the curcumin loading and its amorphous transformation, DTA-TG (see Figure S2a in the Supporting Information) measurements were also carried out, which indicated the absence of the endothermic peak in TNE-Cur. The disappearance of typical curcumin melting point (∼220 °C) actually approved the amorphous state of curcumin in the resulting nanoexcipient formulation. Chemical modification during synthetic and drug loading procedures were probed using infrared spectroscopic (IR) technique (see Figure S2b in the Supporting Information). All samples of TNE showed a broad peak at 3440 cm^{-1}, which were probably ascribed to the free hydroxyl group of phenol and alcohol because of silica and $Ca(OH)_2$. Curcumin is typically characterized by two C═O stretching bands at 1630 and 1560 cm^{-1}, but after complex formation with divalent calcium, these bands are red-shifted to lower wavenumbers, indicating the involvement of carbonyl groups of the curcumin in the chelation to divalent calcium. Moreover, the appearance of additional bands ranges between 1000 and 1700 cm^{-1} indicated the successful loading of curcumin in TNE.

N_2 adsorption/desorption investigation is invariably performed to probe porous structures. Figure 3 illustrates type IV isotherms for MSNs samples, suggesting the existence of mesoporous structures. However, the incorporation of $Ca(OH)_2$ and curcumin loading had a significant impact on gas adsorption results. For instance, the BET surface area of MSNs, TNE, and TNE-Cur was gradually reduced from 728.5 to 411.2

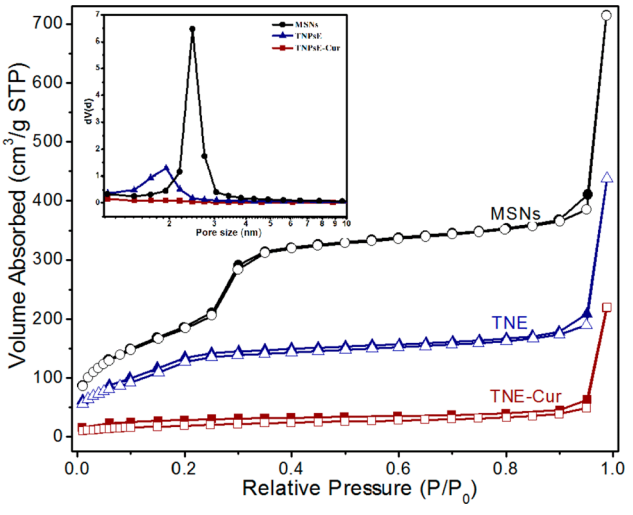

Figure 3. Nitrogen adsorption−desorption isotherms for MSN functionalized with carboxyl groups, TNE, and TNE-Cur. Inset: corresponding pore size distribution curve from adsorption branch.

and 70.7 cm^2 g^{-1}, respectively. Likewise, the pore volume and sizes were decreased from 1.238 to 0.736 and 0.348 cc/g and 2.456 to 1.938 and 1.137 nm, respectively (see Table S1 in the Supporting Information). These findings suggest that the calcium hydroxide encapsulation and significantly high loading of curcumin molecules into porous structure.

Figure S3 shows the XPS findings of resulting curcumin loaded theranostic nanoexcipient; survey spectrum indicates that our sample is mainly consisted of silicon, oxygen, calcium, manganese, and carbon. The C_{1S} spectrum was readily deconvoluted into three fitting curves at 285, 286, and 287 eV which were assigned to C−C, C═O and C═C groups, respectively. Similarly, peaks at 530.5, 531.6, and 533 eV were assigned to the carbonyl oxygen of COOH, C−O, and C═O, suggesting the presence of curcumin molecules in theranostic nanoexcipient. The two main signals in manganese region at 642.9 and 653.7 eV were found, which are in agreement with previous reports and verified the presence of paramagnetic Mn_3O_4 nanoparticles. As far as calcium is concerned, a prominent Ca 2p peak at 347.3 and a weak peak at 351.0 eV are assigned to calcium.

Fluorescence and UV−vis absorption spectroscopy was performed to validate the drug loading in $Ca(OH)_2$ encapsulated MSNs via Ca^{2+}-curcumin coordinate bonding. Figure 4a shows the UV−vis spectra of curcumin and its nanoexcipient complex, pure curcumin showed a main absorption band in UV−vis region (415−430 nm), due to $\pi \rightarrow \pi^*$ transition, however after complex formation this characteristic peak was shifted to a slightly higher energy. A new band at about 475 nm can be observed in the complexes spectra, indicating the participation of carbonyl group of curcumin in metal complexation.[37]

Fluorescence spectra of pure curcumin exhibit a broad and intense fluorescence peak between 440 and 700 nm with excitation of 420 nm (Figure 4b). Fluorescence intensity of fixed amount of curcumin was correspondingly decreased with increasing the nanoexcipient amount, which proved the interaction of curcumin with $Ca(OH)_2$ loaded nanoexcipient. It is well documented that curcumin chelated with several metal ions by β-diketone moiety result fluorescence quench.[38] Accordingly, a color change of curcumin from light yellow to dark red was also observed after mixing with the newly made nanoexcipient and at the same time fluorescence of curcumin was quenched as can be seen UV photograph in the inset of Figure 4a. When pH was lowered to 5.0, a dark red colored solution was transformed to light yellow and fluorescence of curcumin was again recovered, suggesting the cleavage of coordinate bond between the drug and the metal ions and resultantly the curcumin molecules released. Besides curcumin complex dissociation, it is worth mentioning that acid-sensitive calcium hydroxide was also degradation in mildly acidic environment. Dissolution of calcium hydroxide was corroborated by using TEM investigation. Micrograph in Figure 2j indicates the clear mesoporous channels of MSNs after exposing to slightly acidic conditions, whereas completely filled pores of MSNs were observed at pH 7.4. Digital photographs inset Figure 4b demonstrate the hydrophobic or water repellent behavior of free curcumin and ensuing improvement in water solubility following the complex formation with nanoexcipient. A significant amount of yellow-colored curcumin particles were settled down after 10 min, however red colored transparent solution of curcumin loaded nanoexcipient remained homogeneous and particles were kept suspended for much longer time,

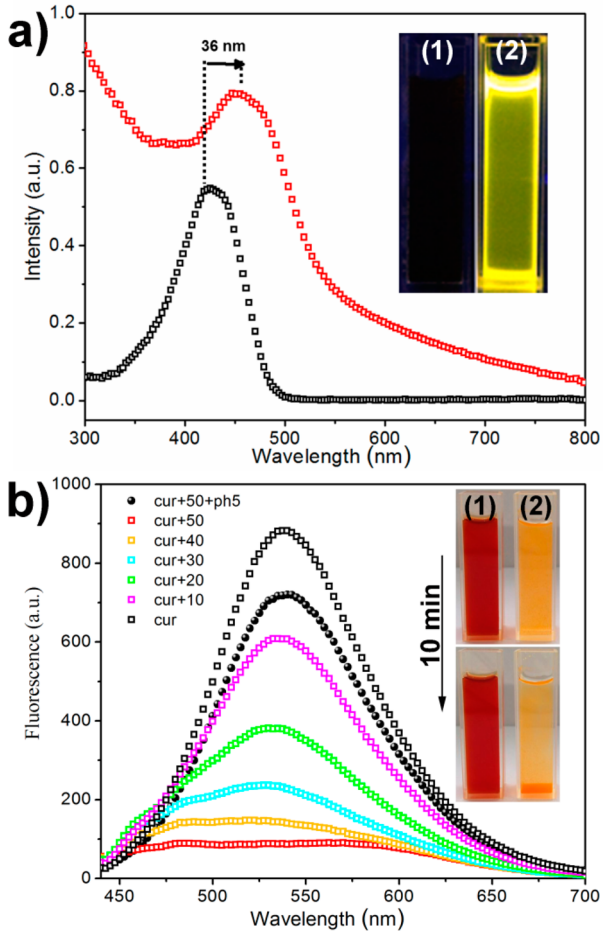

Figure 4. (a) Absorbance spectra of curcumin (black) and TNE added (red) aqueous solutions. Inset: photograph under UV light (365 nm), TNE-Cur (1), Cur (2). (b) Fluorescence spectra of curcumin with the increase of the TNE concentration from 10 to 50 μg. The solid round spectrum is in the presence of ph 5. Inset: photograph of TNE-Cur (1) and curcumin (2) dispersed in water, after 10 min curcumin start precipitate.

and thus chelate formation tendency of curcumin with highly biocompatible calcium hydroxide significantly enhanced the low water solubility limitation of highly promising curcumin.

Targeted and on demand drug delivery to tumor sites is indeed an ideal therapeutic approach to improve the therapeutic index of highly cytotoxic chemotherapeutic drugs. Among various stimuli responsive drug delivery systems, acid sensitive nanoexcipients have been considered a highly desirable feature for effective anticancer drug delivery system because of the existence of mildly acidic extracellular and intracellular microenvironment.[39,40] We evaluated the curcumin release at different pH, Figure 5 revealed a negligible drug release at pH 7.4 (physiological conditions). However, when the pH value was successively lowered to 6.0 (mimicking tumor tissues) and pH 4.5 (mimicking lysosomal condition), a progressive increase in drug release was noticed. This drug release profile verified the $Ca(OH)_2$ and chelates dissociation phenomenon, which consequently led to release of curcumin molecules. Release of curcumin was monitored via UV/vis spectroscopy, whereas the degradation of $Ca(OH)_2$ was determined using Ithe CP-AOS analytical approach. The release of Ca ions corresponded with decreasing pH value,

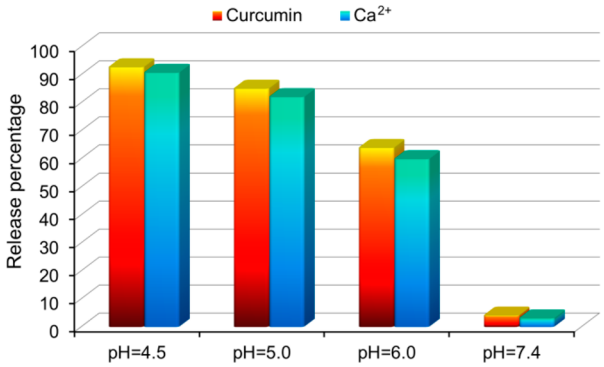

Figure 5. TNE-Cur release of curcumin and Ca^{2+} profile within 30 min in different pH buffer solutions.

and as such, the amount of released calcium correspondingly increased with decreasing pH conditions.

To demonstrate the diagnostic functionality of our resulting theranostic nanoexipient, T1-weighted MRI images of TNE were acquired using 3 T clinical MRI scanners (Figure 6).

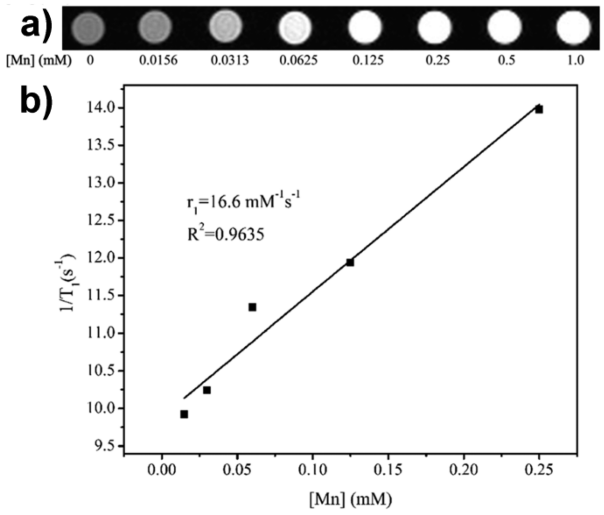

Figure 6. (a) Plot of T_1 relaxation rate ($1/T_1$) versus Mn concentration. (b) T_1-weighted MR images of dispersed NTE at different Mn concentrations in 0.5% agarose.

Different concentrations of manganese conjugated MSNs nanoparticles were dispersed in agar solutions and their contrast enhancement ability was determined. As the concentration of manganese ions was increased, the T1-weighted MR images became brighter and the T1 relaxation time was shortened. The r1 value of the nanoexipient was calculated to be 16.6 mM^{-1} s^{-1}. MRI data show that our theranostic nanoexcipient can be used as imaging probe for magnetic resonance imaging for simultaneous T1MR imaging and targeted release of curcumin.

Numerous recent studies have indicated that curcumin can down-regulate and control gene products of inflammatory transcription factor, nuclear factor-κB activation (NF-κB, constitutively active in patients with pancreatic cancer), and inhibition of cell growth associated with apoptosis.[41−45] To explore the therapeutic significance of these research findings, we performed conventional MTT assay (Figure 7). Various nanoformulations of curcumin were tested against pancreatic cancer cells by incubating for 48 h. As biocompatibility is one of

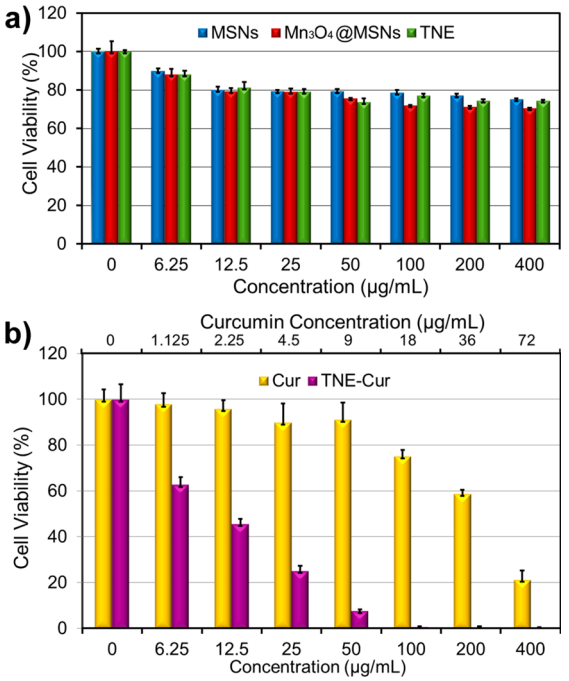

Figure 7. (a) In vitro viability of BxPC-3 cells in the presence of MSNs, Mn_3O_4@MSNs and TNE. (b) TNE-Cur and free curcumin incubation for 48 h. Values are the average of three separate experiments in triplicate and are expressed as mean + SD $*p < 0.05$.

the most basic and crucial factors for any excipient, therefore the biocompatibility of excipient was first determined. MSNs, Mn_3O_4@ MSNs, and $Ca(OH)_2$ encapsulated nanoformulations TNE were found nontoxic at as high as 400 μg/mL concentration, indicating a good biocompatibility of our nanoexcipient. However, a significantly growth inhibition of BxPC-3 cells was observed when cells were treated with suspension of curcumin loaded TNE-Cur formulation.

Compared with the free curcumin, the IC_{50} (concentration of drug formulation required to kill 50% of the cells in a given period) value of nanoformulation was found to be 1.67 μg/mL, whereas the IC_{50} of free curcumin was 29.72 μg/mL. These results indicate the superior antiproliferative activity of chelated curcumin. Such enhanced antitumor effect of formulated curcumin can most likely be attributed to better water solubility and improved cellular internalization because of th enanosize effect. Endocytosis and intracellular release of curcumin was corroborated via confocal fluorescence imaging. A definite amount of developed nanoformulation was incubated for different durations of time. Figure 8 demonstrated that curcumin formulation was successfully taken up by BxPC-3 cells, and it is worth noting that even 1 h of incubation of curcumin nanoformulation showed a higher fluorescence signal than that of free curcumin after 4 h of incubation. Increasing incubation time resulted in a sharp increase in the cell fluorescence. Imaging findings demonstrated a higher intracellular uptake and significant release from curcumin nanoformulation compared to free form of the same drug, thus indirectly verifying 17 times higher cytotoxicity of drug nanoformulation compared to free curcumin.

In conclusion, we have developed a highly biocompatible nanoscale excipient, calcium hydroxide encapsulated mesoporous silica, to deliver hydrophobic curcumin in response to mildly acidic environmental conditions. To impart diagnostic

dx.doi.org/10.1021/am503655z | ACS Appl. Mater. Interfaces 2014, 6, 14377−14383

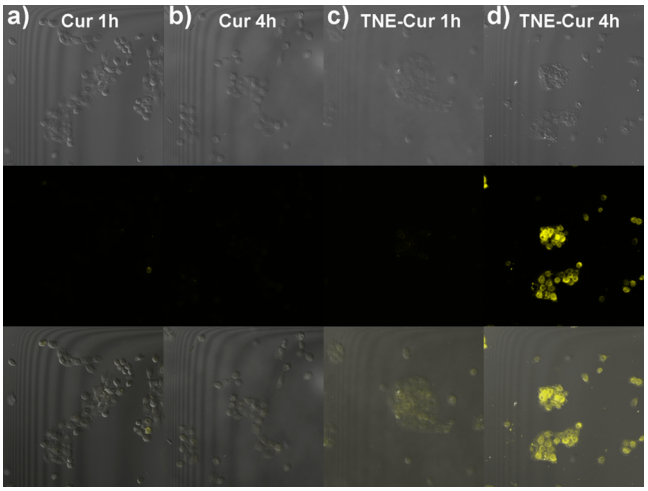

Figure 8. Fluorescence confocal images of curcumin and TNE-Cur uptake by BxPC-3 cancer cells in 1 and 4 h. From top to bottom: bright-field image, fluorescence image, and merged image.

functionality, we also an emergent T1 nanocontrast agent (Mn_3O_4) incorporated into nanoscaffolding. Notably, the presence of divalent calcium into the porous architecture ensured the loading of curcumin molecules through the formation of a chelate between electron-rich carbonyl groups of curcumin and electron deficient metal ions. Subsequently, because of the acid-sensitive nature of calcium hydroxide, loaded curcumin was rapidly released from the porous silica in a mildly acidic environment upon degrading calcium hydroxide excipient. Taken together, a pronounced increase in the apparent solubility of curcumin and acid responsive drug release expectedly demonstrated an excellent cell growth inhibitory performance. A 17-fold increase in chemotherapeutic activity against antipancreatic cancer cell (BxPC-3) was observed when nanoformulation of curcumin was used compared to free drug. We anticipate that the resulting theranostic system can enable more widespread use of curcumin and improve the potential of nano-based medicines.

■ ASSOCIATED CONTENT

Ⓢ Supporting Information

Experimental section and additional figures. This material is available free of charge via the Internet at http://pubs.acs.org.

■ AUTHOR INFORMATION

Corresponding Author

*E-mail: zhugs@jlu.edu.cn.

Notes

The authors declare no competing financial interest.

■ ACKNOWLEDGMENTS

We are grateful to the financial support from National Basic Research Program of China (973 Program, Grant 2012CB821700), Major International (Regional) Joint Research Project of NSFC (Grant 21120102034) NSFC (Grant 20831002), and Australian Research Council Future Fellowship (FT100101059).

■ REFERENCES

(1) Jia, L. Nanoparticle Formulation Increases Oral Bioavailability of Poorly Soluble Drugs: Approaches, Experimental Evidences and Theory. *Curr. Nanosci.* **2005**, *1*, 237−243.
(2) Fahr, A.; Liu, X. Drug Delivery Strategies for Poorly Water-Soluble Drugs. *Exp. Opin. Drug Delivery* **2007**, *4*, 403−416.
(3) Vasconcelos, T.; Sarmento, B.; Costa, P. Solid Dispersions as Strategy to Improve Oral Bioavailability of Poor Water Soluble Drugs. *Drug Discovery Today* **2007**, *12*, 1068−1075.
(4) Vasir, J. K.; Reddy, M. K.; Labhasetwar, V. D. Nanosystems in Drug Targeting: Opportunities and Challenges. *Curr. Nanosci.* **2005**, *1*, 47−64.
(5) Spletstoser, J. T.; Turunen, B. J.; Desino, K.; Rice, A.; Datta, A.; Dutta, D.; Huff, J. K.; Himes, R. H.; Audus, K. L.; Seelig, A.; Georg, G. I. Single-Site Chemical Modification at C10 of the Baccatin III Core of Paclitaxel and Taxol C Reduces P-glycoprotein Interactions in Bovine Brain Microvessel Endothelial Cells. *Bioorg. Med. Chem. Lett.* **2006**, *16*, 495−498.
(6) Rice, A.; Liu, Y. B.; Michaelis, M. L.; Himes, R. H.; Georg, G. I.; Audus, K. L. Chemical Modification of Paclitaxel (Taxol) Reduces P-glycoprotein Interactions and Increases Permeation across the Blood-Brain Barrier in Vitro and in Situ. *J. Med. Chem.* **2005**, *48*, 832−838.
(7) Kesisoglou, F.; Panmai, S.; Wu, Y. Nanosizing-Oral Formulation Development and Biopharmaceutical Evaluation. *Adv. Drug Delivery Rev.* **2007**, *59*, 631−44.
(8) Yen, F. L.; Wu, T. H.; Tzeng, C. W.; Lin, L. T.; Lin, C. C. Curcumin Nanoparticles Improve the Physicochemical Properties of Curcumin and Effectively Enhance its Antioxidant and Antihepatoma Activities. *J. Agric. Food Chem.* **2010**, *58*, 7376−82.
(9) Duncan, R. The Dawning Era of Polymer Therapeutics. *Nat. Rev. Drug Discovery* **2003**, *2*, 347−360.
(10) Merisko-Liversidge, E. M.; Liversidge, G. G. Drug Nanoparticles: Formulating Poorly Water-Soluble Compounds. *Toxicol. Pathol.* **2008**, *36*, 43−48.
(11) Porter, C. J. H.; Pouton, C. W.; Cuine, J. F.; Charman, W. N. Enhancing Intestinal Drug Solubilisation Using Lipid-Based Delivery Systems. *Adv. Drug Delivery Rev.* **2008**, *60*, 673−691.
(12) Hauss, D. J. Oral Lipid-Based Formulations. *Adv. Drug Delivery Rev.* **2007**, *59*, 667−676.
(13) Chen, M. C.; Tsai, H. W.; Liu, C. T.; Peng, S. F.; Lai, W. Y.; Chen, S. J.; Chang, Y.; Sung, H. W. A Nanoscale Drug-Entrapment Strategy for Hydrogel-Based Systems for the Delivery of Poorly Soluble Drugs. *Biomaterials* **2009**, *30*, 2102−2111.
(14) Goldsipe, A.; Blankschtein, D. Molecular-Thermodynamic Theory of Micellization of Multicomponent Surfactant Mixtures: 1. Conventional (pH-Insensitive) Surfactants. *Langmuir* **2007**, *23*, 5942−5952.
(15) Bhat, P. A.; Dar, A. A.; Rather, G. M. Solubilization Capabilities of some Cationic, Anionic, and Nonionic Surfactants toward the Poorly Water-Soluble Antibiotic Drug Erythromycin. *J. Chem. Eng. Data* **2008**, *53*, 1271−1277.
(16) Torchilin, V. P. Targeted Polymeric Micelles for Delivery of Poorly Soluble Drugs. *Cell. Mol. Life. Sci.* **2004**, *61*, 2549−2559.
(17) Lu, J.; Liong, M.; Zink, J. I.; Tamanoi, F. Mesoporous Silica Nanoparticles as a Delivery System for Hydrophobic Anticancer Drugs. *Small* **2007**, *3*, 1341−1346.
(18) Rosenholm, J. M.; Sahlgren, C.; Linden, M. Towards Multifunctional, Targeted Drug Delivery Systems Using Mesoporous Silica Nanoparticles - Opportunities & Challenges. *Nanoscale* **2010**, *2*, 1870−1883.
(19) Li, Z. X.; Barnes, J. C.; Bosoy, A.; Stoddart, J. F.; Zink, J. I. Mesoporous Silica Nanoparticles in Biomedical Applications. *Chem. Soc. Rev.* **2012**, *41*, 2590−2605.
(20) Mellaerts, R.; Jammaer, J. A. G.; Van Speybroeck, M.; Chen, H.; Van Humbeeck, J.; Augustijns, P.; Van den Mooter, G.; Martens, J. A. Physical State of Poorly Water Soluble Therapeutic Molecules Loaded into SBA-15 Ordered Mesoporous Silica Carriers: A Case Study with Itraconazole and Ibuprofen. *Langmuir* **2008**, *24*, 8651−8659.

(21) Sharma, R. A.; Gescher, A. J.; Steward, W. P. Curcumin: The Story so far. *Eur. J. Cancer* **2005**, *41*, 1955−1968.
(22) Yallapu, M. M.; Jaggi, M.; Chauhan, S. C. Curcumin Nanoformulations: A Future Nanomedicine for Cancer. *Drug Discovery Today* **2012**, *17*, 71−80.
(23) Luer, S.; Troller, R.; Jetter, M.; Spaniol, V.; Aebi, C. Topical Curcumin can Inhibit Deleterious Effects of Upper Respiratory Tract Bacteria on Human Oropharyngeal Cells in Vitro: Potential Role for Patients with Cancer Therapy Induced Mucositis? *Support Care Cancer* **2011**, *19*, 799−806.
(24) Shishodia, S.; Chaturvedi, M. M.; Aggarwal, B. B. Role of Curcumin in Cancer Therapy. *Curr. Probl. Cancer* **2007**, *31*, 243−305.
(25) Esatbeyoglu, T.; Huebbe, P.; Ernst, I. M.; Chin, D.; Wagner, A. E.; Rimbach, G. Curcumin−From Molecule to Biological Function. *Angew. Chem., Int. Ed.* **2012**, *51*, 5308−32.
(26) Takahashi, M.; Uechi, S.; Takara, K.; Asikin, Y.; Wada, K. Evaluation of an Oral Carrier System in Rats: Bioavailability and Antioxidant Properties of Liposome-Encapsulated Curcumin. *J. Agric. Food Chem.* **2009**, *57*, 9141−9146.
(27) Sun, D. M.; Zhuang, X. Y.; Xiang, X. Y.; Liu, Y. L.; Zhang, S. Y.; Liu, C. R.; Barnes, S.; Grizzle, W.; Miller, D.; Zhang, H. G. A Novel Nanoparticle Drug Delivery System: The Anti-inflammatory Activity of Curcumin Is Enhanced When Encapsulated in Exosomes. *Mol. Ther.* **2010**, *18*, 1606−1614.
(28) Gou, M. L.; Men, K.; Shi, H. S.; Xiang, M. L.; Zhang, J. A.; Song, J.; Long, J. L.; Wan, Y.; Luo, F.; Zhao, X.; Qian, Z. Y. Curcumin-Ioaded Biodegradable Polymeric Micelles for Colon Cancer Therapy in Vitro and in Vivo. *Nanoscale* **2011**, *3*, 1558−1567.
(29) Chin, S. F.; Iyer, K. S.; Saunders, M.; St Pierre, T. G.; Buckley, C.; Paskevicius, M.; Raston, C. L. Encapsulation and Sustained Release of Curcumin using Superparamagnetic Silica Reservoirs. *Chem.—Eur. J.* **2009**, *15*, 5661−5665.
(30) Wang, X. J.; Chen, D. H.; Cao, L.; Li, Y. C.; Boyd, B. J.; Caruso, R. A. Mesoporous Titanium Zirconium Oxide Nanospheres with Potential for Drug Delivery Applications. *ACS Appl. Mater. Interfaces* **2013**, *5*, 10926−10932.
(31) Clifford, N. W.; Iyer, K. S.; Raston, C. L. Encapsulation and Controlled Release of Nutraceuticals using Mesoporous Silica Capsules. *J. Mater. Chem.* **2008**, *18*, 162−165.
(32) Jin, D.; Park, K. W.; Lee, J. H.; Song, K.; Kim, J. G.; Seo, M. L.; Jung, J. H. The Selective Immobilization of Curcumin onto the Internal Surface of Mesoporous Hollow Silica Particles by Covalent Bonding and its Controlled Release. *J. Mater. Chem.* **2011**, *21*, 3641−3645.
(33) Yan, H.; Teh, C.; Sreejith, S.; Zhu, L. L.; Kwok, A.; Fang, W. Q.; Ma, X.; Nguyen, K. T.; Korzh, V.; Zhao, Y. L. Functional Mesoporous Silica Nanoparticles for Photothermal-Controlled Drug Delivery In Vivo. *Angew. Chem., Int. Ed.* **2012**, *51*, 8373−8377.
(34) Zhao, Y. N.; Trewyn, B. G.; Slowing, I. I.; Lin, V. S. Y. Mesoporous Silica Nanoparticle-Based Double Drug Delivery System for Glucose-Responsive Controlled Release of Insulin and Cyclic AMP. *J. Am. Chem. Soc.* **2009**, *131*, 8398−8400.
(35) Patel, A.; Hu, Y. C.; Tiwari, J. K.; Velikov, K. P. Synthesis and Characterisation of Zein-Curcumin Colloidal Particles. *Soft Matter* **2010**, *6*, 6192−6199.
(36) Guo, M. Y.; Muhammad, F.; Wang, A. F.; Qi, W. X.; Wang, N.; Guo, Y. J.; Wei, Y.; Zhu, G. S. Magnesium Hydroxide Nanoplates: A pH-Responsive Platform for Hydrophobic Anticancer Drug Delivery. *J. Mater. Chem. B* **2013**, *1*, 5273−5278.
(37) Song, Y. M.; Xu, J. P.; Ding, L.; Hou, Q.; Liu, J. W.; Zhu, Z. L. Syntheses, Characterization and Biological Activities of Rare Earth Metal Complexes with Curcumin and 1,10-phenanthroline-5,6-dione. *J. Inorg. Biochem.* **2009**, *103*, 396−400.
(38) Zebib, B.; Mouloungui, Z.; Noirot, V. Stabilization of Curcumin by Complexation with Divalent Cations in Glycerol/Water System. *Bioinorg Chem. Appl.* **2010**.
(39) Samal, S. K.; Dash, M.; Van Vlierberghe, S.; Kaplan, D. L.; Chiellini, E.; van Blitterswijk, C.; Moroni, L.; Dubruel, P. Cationic Polymers and Their Therapeutic Potential. *Chem. Soc. Rev.* **2012**, *41*, 7147−7194.
(40) Rothstein, S. N.; Little, S. R. A "Tool Box" for Rational Design of Degradable Controlled Release Formulations. *J. Mater. Chem.* **2011**, *21*, 29−39.
(41) Dhillon, N.; Aggarwal, B. B.; Newman, R. A.; Wolf, R. A.; Kunnumakkara, A. B.; Abbruzzese, J. L.; Ng, C. S.; Badmaev, V.; Kurzrock, R. Phase II trial of Curcumin in Patients with Advanced Pancreatic Cancer. *Clin. Cancer Res.* **2008**, *14*, 4491−4499.
(42) Dandawate, P. R.; Vyas, A.; Ahmad, A.; Banerjee, S.; Deshpande, J.; Swamy, K. V.; Jamadar, A.; Dumhe-Klaire, A. C.; Padhye, S.; Sarkar, F. H. Inclusion Complex of Novel Curcumin Analogue CDF and beta-Cyclodextrin (1:2) and Its Enhanced In Vivo Anticancer Activity Against Pancreatic Cancer. *Pharm. Res.* **2012**, *29*, 1775−1786.
(43) Ali, S.; Ahmad, A.; Banerjee, S.; Padhye, S.; Dominiak, K.; Schaffert, J. M.; Wang, Z. W.; Philip, P. A.; Sarkar, F. H. Gemcitabine Sensitivity Can Be Induced in Pancreatic Cancer Cells through Modulation of miR-200 and miR-21 Expression by Curcumin or Its Analogue CDF. *Cancer Res.* **2010**, *70*, 3606−3617.
(44) Raju, G. S. R.; Pavitra, E.; Nagaraju, G. P.; Ramesh, K.; El-Rayes, B. F.; Yu, J. S. Imaging and Curcumin Delivery in Pancreatic Cancer Cell lines Using PEGylated Alpha-Gd-2(MoO4)(3) Mesoporous Particles. *Dalton Trans.* **2014**, *43*, 3330−3338.
(45) Nagaraju, G. P.; Zhu, S. J.; Wen, J.; Farris, A. B.; Adsay, V. N.; Diaz, R.; Snyder, J. P.; Mamoru, S.; El-Rayes, B. F. Novel Synthetic Curcumin Analogues EF31 and UBS109 are Potent DNA Hypomethylating Agents in Pancreatic Cancer. *Cancer Lett.* **2013**, *341*, 195−203.